Time-Reversal Symmetry Bounds on the Electromagnetic Response of Asymmetric Structures

Dimitrios L. Sounas and Andrea Alù*
Department of Electrical and Computer Engineering, The University of Texas at Austin, Austin, Texas 78712, USA
(Received 13 September 2016; published 14 April 2017)

Asymmetric structures support different field distributions and electromagnetic responses when excited from different directions. Here we show that time-reversal symmetry imposes fundamental constraints on their overall response, beyond those dictated by reciprocity. For two-port devices, the asymmetry in field distribution for opposite excitations is shown to be fundamentally bounded by the reflection at the ports, and the fields are identical everywhere in space in the case of full transmission. In multiport and open scenarios, these bounds have implications on radiation and scattering at different ports and towards different directions. Beyond their theoretical significance, these results provide relevant insights into the operation of nonlinear isolators, metasurfaces, and other nanophotonic devices.

DOI: 10.1103/PhysRevLett.118.154302

The symmetry of various physical laws under time reversal is at the basis of many physical principles [1]. In simple terms, time-reversal symmetry implies that the response of a system under a $t \to -t$ transformation satisfies the same physical laws as the original system. For example, the time-reversed response of a time-reversal invariant electromagnetic system is always a solution of Maxwell equations in the same system. The most important consequence in classical systems is reciprocity, according to which signal transmission between two points in space is the same for both propagation directions [2–5], recently inspiring the realization of magnetless electromagnetic and acoustic nonreciprocal devices for full-duplex communication systems [6–24].

Here, we discuss how time-reversal symmetry imposes even stricter constraints on the operation of electromagnetic systems, beyond reciprocity. In particular, we show that in arbitrarily asymmetric volumes local quantities such as the field intensity and the radiated power from point sources cannot take arbitrary values when the structure is probed from different directions. We start our analysis with the simple scenario of a two-port lossless structure [Fig. 1(a)], and then move to the case of multiport structures [Fig. 1(b)], and to objects in free space [Fig. 1(c)]. In all these scenarios, we show that the degree of asymmetry in their electromagnetic response decreases as the transmission coefficient increases, and it vanishes in the case of perfect transmission. We conclude our paper discussing several practical consequences of these findings, such as in the operation of nonlinear isolators and the cloaking of directive emitters.

Consider an arbitrary two-port, lossless, and linear network, as in Fig. 1(a), with transmission coefficient T (equal when excited from the two ports, due to reciprocity) and reflection coefficients R_1 and R_2 at ports 1 and 2, respectively. Since the network is lossless, $|R_1|=|R_2|=R$. Let the field distribution inside the structure be $\mathbf{E}_1(\mathbf{r})$ and $\mathbf{E}_2(\mathbf{r})$ when excited from ports 1 and 2 with signals of unitary amplitude, respectively. If we apply a time-reversal operation to the case in which the structure is excited from port 1 [top, Fig. 1(a)], we obtain an inversion of the propagation direction for all impinging, reflected, and transmitted waves, a complex conjugation of the amplitudes of these waves, and a complex conjugation of the induced field distribution, leading to the scenario shown in the bottom of Fig. 1(a). Since the structure is lossless, and assuming it is time-invariant and it is not biased by any quantity that is odd symmetric under time reversal, the internal field $\mathbf{E}_1^*$ in the time-reversed scenario can be expressed as a superposition of the fields in the original scenario as $\mathbf{E}_1^* = R_1^*\mathbf{E}_1 + T^*\mathbf{E}_2$. After some algebraic manipulations [25] (Sec. I), we find

$$\frac{1-R}{1+R} \le \frac{|\mathbf{E}_2|^2}{|\mathbf{E}_1|^2} \le \frac{1+R}{1-R}. \tag{1}$$

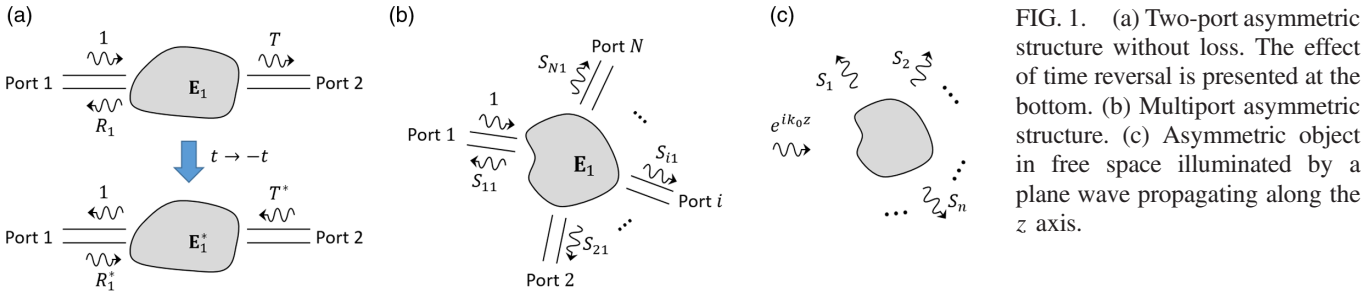

FIG. 1. (a) Two-port asymmetric structure without loss. The effect of time reversal is presented at the bottom. (b) Multiport asymmetric structure. (c) Asymmetric object in free space illuminated by a plane wave propagating along the z axis.

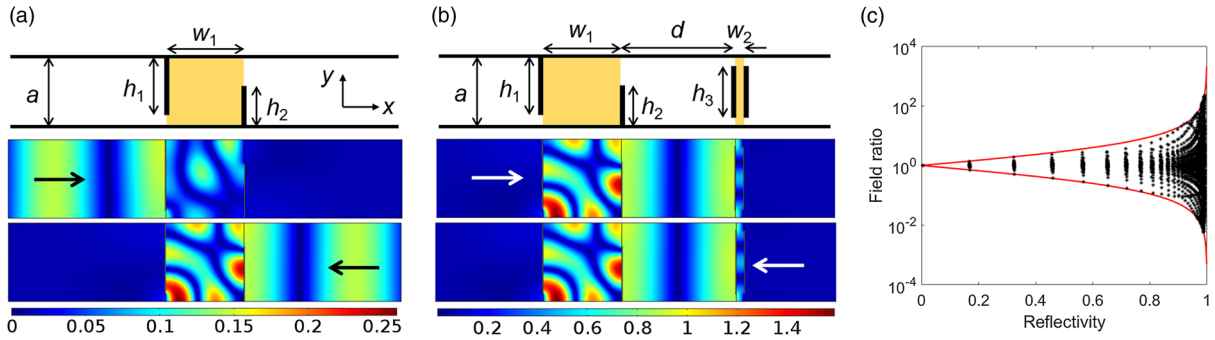

FIG. 2. Numerical validation of the time-reversal-symmetry bound for two-port structures. (a) Multimodal cavity inside a parallel-plate waveguide. All the walls are PEC and the material of the cavity has $\varepsilon_r = 12$. The cavity parameters are $h_1 = 0.9a$, $h_2 = 0.7a$, $w_1 = a$. The operation frequency is $0.35c/a$ and the electric field is polarized along the y axis with amplitude 1 V/m. (b) Same as in (a), but with an additional matching layer at the right-hand side of the cavity, which consists of metallic patches on both sides of a dielectric substrate with permittivity $\varepsilon_r = 12$. The parameters are $d = 1.449a$, $w_2 = 0.1a$, and $h_3 = 0.81a$. The color bar scale is different than in (a) in order to properly show the details of the fields, which are stronger in this case. (c) Field ratio versus reflectivity for excitation from opposite sides for the structure in (b) at 25 equally distributed points inside the cavity and 101 equally distributed frequencies over a band centered at frequency $0.35c/a$ and with width $0.03c/a$. The red lines correspond to the upper and lower bounds in Eq. (1) for the field intensity ratio. All simulations have been performed with COMSOL MULTIPHYSICS.

Equation (1) shows that the ratio of field intensities at any point inside the structure for excitation from different ports is bounded by quantities that tend to unity as the reflection at the input ports decreases (or the transmission increases). In the extreme case of perfect transmission, the internal field intensity distribution for excitation from opposite directions is exactly the same anywhere, independent of the geometrical asymmetry and complexity of the structure. An analogous expression to Eq. (1) was derived in [26] for the decay rates at different ports of a two-port single-resonance system. It is possible to show [25] (Sec. II) that this result is a particular case of Eq. (1), and our theory extends it to generally complex asymmetric structures, without the single-resonance restriction, at any frequency and, quite surprisingly, to any single point in space.

In order to validate Eq. (1), we have simulated an asymmetric two-port system consisting of a multimodal cavity inside a parallel-plate waveguide, as in Fig. 2(a). The walls of the waveguide and the cavity are perfect electric conductors (PEC) and the cavity is filled with a high-permittivity dielectric ($\varepsilon_r = 12$). The structure's asymmetry is achieved through apertures of different width and position at opposite sides of the cavity. We excite at a frequency where reflection is nonzero, as it can be deduced from the standing-wave patterns on the side of the waveguide from which the excitation is applied. In this case, the fields for excitation from opposite sides are very different, as expected in an asymmetric multimodal cavity. Then, one may wonder whether it is possible to maintain this field asymmetry while increasing the transmission coefficient through the structure. Without changing the geometrical asymmetry, we add a matching layer in the form of a reactive surface, consisting of identical metallic patches on either side of a thin dielectric layer, at some distance from the right-hand side of the cavity, as in Fig. 2(b). By controlling the geometry of the antireflection surface and its distance from the cavity, it is possible to impedance match the asymmetric cavity to the waveguide and achieve unitary transmission (zero reflection). Because of reciprocity, the matching works for excitation from either side. Despite the fact that we have not modified the original asymmetry of the system, the field intensity profile for excitation from opposite directions is now identical at any point in the waveguide, in full agreement with Eq. (1) for $R = 0$, showing that the bounds in Eq. (1) are not related to geometrical asymmetries, but they are a fundamental consequence of time-reversal symmetry. Finally, Fig. 2(c) presents $|\mathbf{E}_2|^2/|\mathbf{E}_1|^2$ versus R for the system in Fig. 2(b), calculated at 25 points inside the cavity for 101 frequency points over a band around the frequency of unitary transmission. The width of this frequency range is chosen so that the reflection coefficient varies from 0 to 1. It can be seen that in all cases and at all points $|\mathbf{E}_2|^2/|\mathbf{E}_1|^2$ lies within the bounds predicted by Eq. (1), validating our theoretical analysis.

Consider now a multiport system, as the one in Fig. 1(b). We first assume zero loss, but, as we rigorously show in [25] (Sec. IV), the derived results also apply to lossy systems, since loss can be interpreted as one of the output ports of a generic multiport network. When the system is excited by a signal with unitary amplitude from port 1, assuming that all ports are matched, the outgoing signal at the nth port has scattering parameter S_{n1}. After applying a time-reversal operation, we can write the field at any point in the structure in the time-reversed scenario as a superposition of the fields induced by impinging signals $S_{n1}^*: \mathbf{E}_1^* = S_{11}^*\mathbf{E}_1 + S_{21}^*\mathbf{E}_2 + \cdots + S_{N1}^*\mathbf{E}_N$, where $\mathbf{E}_n$ is the field for excitation from the nth port. After some algebraic manipulations [25] (Sec. III), we find $(|\mathbf{E}_1|^2/\sum|\mathbf{E}|^2) + (|\mathbf{E}_2|^2/\sum|\mathbf{E}|^2) - 2|S_{21}|(|\mathbf{E}_1|/\sqrt{\sum|\mathbf{E}|^2})(|\mathbf{E}_2|/\sqrt{\sum|\mathbf{E}|^2}) \leq 1 - |S_{21}|^2$, where $\sum|\mathbf{E}|^2 = |\mathbf{E}_1|^2 + |\mathbf{E}_2|^2 + \cdots + |\mathbf{E}_N|^2$.

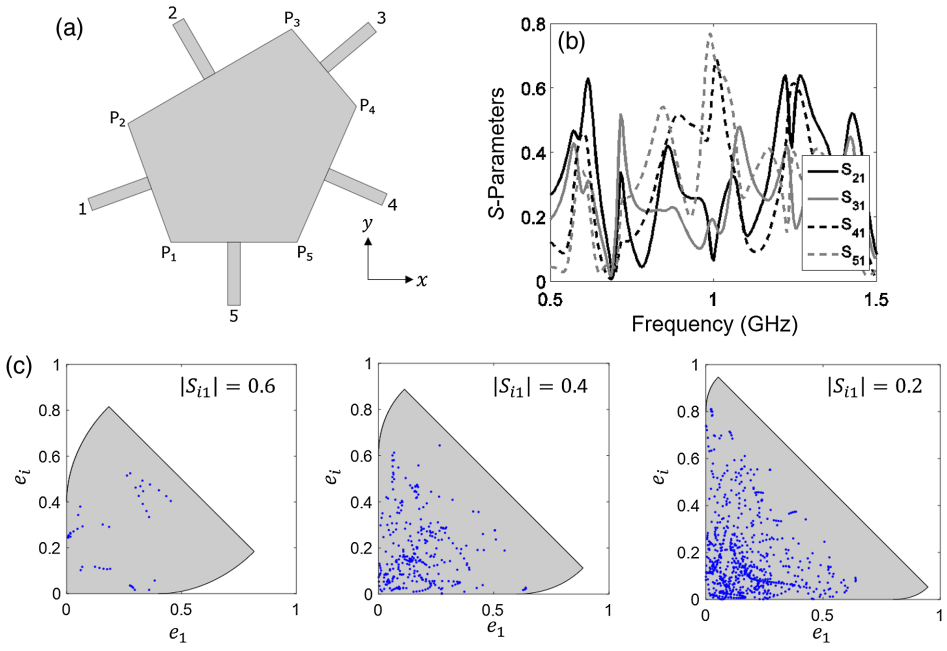

FIG. 3. Multiport and multimodal asymmetric structure. (a) The structure is infinitely extended along the z direction, is filled with air, and has PMC walls. The cavity vertices are $P_1 = (0,0)$ m, $P_2 = (-0.1, 0.28)$ m, $P_3 = (0.29, 0.51)$ m, $P_4 = (0.44, 0.32)$ m, and $P_5 = (0.3, 0)$ m. The width of the external channels is 0.03 m. (b) S parameters for excitation from port 1. (c) Radiation efficiency at different ports for a dipole source located at six different evenly distributed points inside the cavity, including the center of mass $O = \sum_{k=1}^{5} P_k/5$ and the midpoints between O and the cavity vertices. The shaded regions correspond to the radiation efficiencies allowed by time-reversal symmetry. The simulations were carried out through COMSOL MULTIPHYSICS for z-polarized incident waves with amplitude 1 V/m and uniform profile across the waveguide cross sections.

Interestingly, $|\mathbf{E}_n|^2$ may be interpreted as the radiated power P_n at the nth port from a randomly oriented dipole source located at the position in which we sample $\mathbf{E}_n$: $P_n = \omega^2|p|^2|\mathbf{E}_n|^2/48$, where p is the dipole moment [25] (Sec. VI). The total radiated power by the dipole is given by $P = \sum_{n=1}^{N} P_n = \omega^2|p|^2\Sigma|\mathbf{E}|^2/24$, yielding

$$e_1 + e_2 - 2|S_{21}|\sqrt{e_1 e_2} \leq 1 - |S_{21}|^2, \qquad (2)$$

where $e_n = P_n/P$ is the radiation efficiency at the nth port. Equation (2) shows that the difference in radiation efficiencies between any two ports is restricted by the transmission coefficient between the same ports. In the case of zero transmission between the ports ($|S_{21}| = 0$), Eq. (2) becomes $e_1 + e_2 \leq 1$ and it is satisfied for any value of e_1 and e_2 allowed by power conservation, indicating that in such a case radiation at different ports is independent. On the other hand, for unitary transmission ($|S_{21}| = 1$), Eq. (2) becomes $e_1 + e_2 - 2\sqrt{e_1 e_2} \leq 0$, and it can be satisfied only for $e_1 = e_2$, indicating full correlation of radiation at the two ports. For intermediate values of $|S_{21}|$, the radiation at different ports is partially correlated, and it increases as $|S_{21}|$ increases. The result in Eq. (2) has relevant implications not only for waveguide problems, but also in the case of optical systems excited by thermal or quantum emitters, and for the design of unidirectional lasers and absorbers without back-reflecting mirrors [29]. Indeed, our theory proves that the energy emitted in different directions by a small emitter is necessarily bound by the way the two directions are coupled together, with relevant implications in nanophotonic engineering. Furthermore, Eq. (2) can be extended to lossy systems [25] (Sec. IV), as it may intuitively be understood from the fact that absorption can be seen as an additional output channel.

We validated these theoretical results using full-wave simulations of a multiport, multimodal asymmetric cavity, as in Fig. 3(a). The structure is two dimensional with perfect-magnetic-conducting (PMC) walls and filled with air. The electric field is assumed to have a single out-of-plane component, and the external waveguides support propagation of only the fundamental transverse electromagnetic mode. Fig. 3(b) shows the calculated S parameters of such a structure for excitation from port 1, showing the existence of multiple resonances and significant asymmetry of transmission at different ports. The large range of values for the transmission coefficient allows validating Eq. (2) for different transmission levels and, therefore, different degrees of correlation for the radiation efficiency of an arbitrarily located point emitter at different ports. Figure 3(c) shows e_1 versus e_n, with $n \neq 1$, for three different values of $|S_{n1}|$. For each value of $|S_{n1}|$, we determine the corresponding frequencies from Fig. 3(b) and simulate the structure at these frequencies assuming an emitter at different points in the cavity. In all cases the radiation efficiency lies within the bounds predicted by Eq. (2) (grey regions).

These multiport bounds have interesting consequences also in the case of periodic metasurfaces designed to tailor thermal or optical emission. In particular, they imply that the difference between the radiation efficiency of a point emitter close to the metasurface along two different directions is restricted by the transmission coefficient S_{21} between these directions. For random directions, $S_{21} = 0$ and no restriction exists. However, if the directions belong

to the set of diffraction orders determined by the metasurface's periodicity, S_{21} is typically nonzero, and e_1 and e_2 are related to each other through Eq. (2). Consider, for instance, a reflective metasurface with periodicity smaller than the diffraction limit. Such a metasurface supports only one diffraction order and, for zero loss, leads to unitary specular reflection for any incidence direction. Then, Eq. (2) implies that a point emitter close to this surface necessarily exhibits the same radiation efficiency for symmetric directions with respect to the normal direction; i.e., the emitter has a symmetric radiation pattern, regardless of any arbitrary asymmetry in the metasurface's unit cell. The multiport bounds in the case of metasurfaces reveal the conditions to obtain directive emission, again with several implications in nanophotonic engineering.

This multiport scenario may be further generalized to the case of a system in free space open to radiation, as in Fig. 1(c). Let $\mathbf{E}(\mathbf{k}_0)$ be the impinging electric field of a plane wave with unitary amplitude, polarization vector $\hat{\boldsymbol{\varepsilon}}_0$, and wave vector $\mathbf{k}_0$. Furthermore, let $S_n(\hat{\boldsymbol{\varepsilon}}_0, \mathbf{k}_0)$ be the amplitude of the nth scattered spherical-wave harmonic, normalized so that $|S_n(\hat{\boldsymbol{\varepsilon}}_0, \mathbf{k}_0)|^2$ is the scattered power carried by the harmonic. Applying a time-reversal transformation to this problem results in a system excited by a plane wave of unitary amplitude, polarization vector $\hat{\boldsymbol{\varepsilon}}_0^*$, and wave vector $-\mathbf{k}_0$, and incoming spherical-wave harmonics with amplitudes $S_n^*(\hat{\boldsymbol{\varepsilon}}_0, \mathbf{k}_0)$. Similar to the case of single- and multiport systems, we get $\mathbf{E}^*(\hat{\boldsymbol{\varepsilon}}_0, \mathbf{k}_0) = \mathbf{E}(\hat{\boldsymbol{\varepsilon}}_0^*, -\mathbf{k}_0) + \sum_n S_n^*(\hat{\boldsymbol{\varepsilon}}_0, \mathbf{k}_0)\mathbf{E}_n$, where $\mathbf{E}_n$ is the field induced by the nth incident harmonic. Performing some algebraic manipulations and considering the definition of radiation gain for an arbitrarily oriented point emitter [28], as detailed in [25] (Sec. VI), yields

$$\frac{\lambda^2}{4\pi}\left[\sqrt{G(\hat{\boldsymbol{\varepsilon}}_0, \mathbf{k}_0)} - \sqrt{G(\hat{\boldsymbol{\varepsilon}}_0^*, -\mathbf{k}_0)}\right]^2 \leq \sigma_{\text{ext}}(\hat{\boldsymbol{\varepsilon}}_0, \mathbf{k}_0) = \sigma_{\text{ext}}(\hat{\boldsymbol{\varepsilon}}_0^*, -\mathbf{k}_0), \tag{3}$$

where $\sigma_{\text{ext}}(\hat{\boldsymbol{\varepsilon}}_0, \mathbf{k}_0)$ is the extinction cross section of the scatterer [1] and $G(\hat{\boldsymbol{\varepsilon}}_0, \mathbf{k})$ is the emitter's gain along the direction $\mathbf{k}$ and for the $\hat{\boldsymbol{\varepsilon}}_0$ polarization of the far field [30]. In Eq. (3) we used $\sigma_{\text{ext}}(\hat{\boldsymbol{\varepsilon}}_0, \mathbf{k}_0) = \sigma_{\text{ext}}(\hat{\boldsymbol{\varepsilon}}_0^*, -\mathbf{k}_0)$, a result of reciprocity [31]. Equation (3) represents an upper bound for the difference in gain for opposite directions—a measure of the scattering directionality of the object—versus the extinction cross section, highlighting a direct relation between radiation and scattering properties of an arbitrary object, stemming from time-reversal symmetry. This limitation may be overcome only using active or nonreciprocal materials.

In order to provide further insights and validate Eq. (3), we analyze the case of an infinite dielectric cylinder excited by a line source, as in Fig. 4(a). Since the structure is circularly symmetric, different field profiles, and subsequently different radiation gain for different directions, can be induced by exciting multiple resonant modes. For this

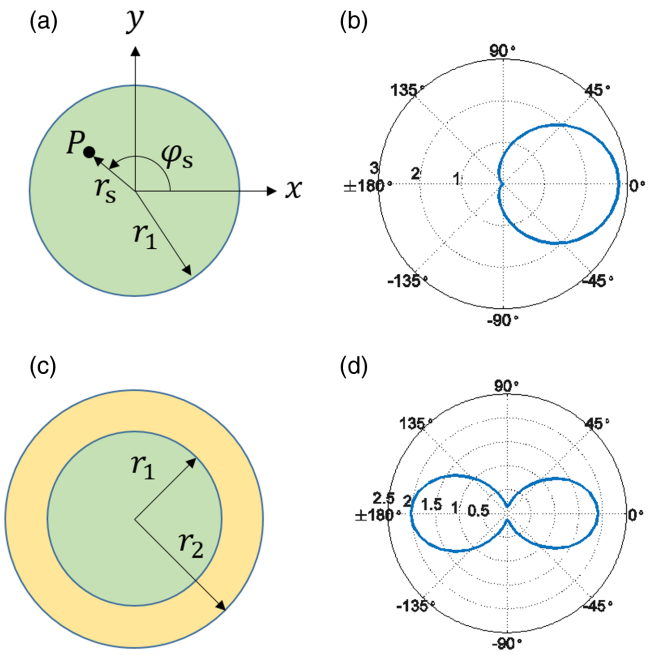

FIG. 4. (a) Circular cylindrical scatterer in free space, with permittivity $\varepsilon_1 = 12$, permeability $\mu_1 = 1$, and radius $r_1 = 0.0795\lambda$, where λ is the free-space wavelength. (b) Radiation pattern for a line source located at point P with polar coordinates $r_s = 0.5r_1$ and $\varphi_s = 180$ deg. (c) The cylinder in (a) covered with a metamaterial shell with permittivity $\varepsilon_2 = -3$, permeability $\mu_2 = -4.5$, and radius $r_2 = 1.45r_1$, resulting in a scattering cross-section reduction from 0.64λ to 0.01λ. (d) Radiation pattern for the same source as in (b), but with the metamaterial cover.

reason, the permittivity and radius of the cylinder are selected to operate between the TM_0 and TM_1 resonances of the cylinder. The corresponding radiation pattern is presented in Fig. 4(b) for a source at $r_s = 0.5r_1$ and $\varphi_s = 180$ deg, showing strong directionality. We now cover the cylinder with a metamaterial shell, as in Fig. 4(c), aimed at suppressing its scattering cross section for z-polarized waves ($\hat{\boldsymbol{\varepsilon}}_0 = \hat{\mathbf{z}}$) [32–34]. From Eq. (3), we expect $G(\mathbf{k}_0) = G(-\mathbf{k}_0)$; i.e., the radiation pattern becomes symmetric in opposite directions. Figure 4(d) shows indeed that the radiation pattern with the metamaterial shell for the same source as in Fig. 4(b) is symmetric, highlighting how cloaking essentially destroys radiation directivity for excitation by an internal point source.

In addition to their theoretical significance, the results presented in this Letter are important from a practical perspective in the design of a plethora of linear and nonlinear nanophotonic devices. As an example of the consequence of these results in nonlinear problems, consider the case of nonlinear isolators, which achieve nonreciprocal transmission based on materials with intensity-dependent permittivity [35–43]. Their operation is based on the fact that, by design, the induced field distribution is asymmetrical for excitation from different ports, and therefore the transmission coefficients for opposite excitations can be made largely different based on the different permittivity

distribution in the device when excited from opposite sides. Large nonreciprocity is induced if, for instance, the structure is designed to operate in a high-intensity, strongly nonlinear regime for one propagation direction, for which the transmission coefficient is very small because of the strong excitation of a resonance, and a low-intensity, quasilinear regime for the other propagation direction, for which the transmission coefficient is large because the resonance is weakly excited. The bounds presented here show that in the low-intensity (linear) regime there is a fundamental trade-off between large transmission and induced field asymmetry, and therefore directly impose fundamental constraints on the insertion loss and transmission contrast of nonlinear isolators, a conclusion consistent with the metrics reported so far in the literature for these devices. We have discussed how the bounds presented here also have implications in the design of directive thermal, optical, and quantum emitters, metasurfaces, lasers, and absorbers, and reveal the extent up to which such systems can be cloaked and at the same time exhibit directional emission properties.

This work was supported by the Air Force Office of Scientific Research (AFOSR), the National Science Foundation (NSF), and the Simons Foundation.

To whom correspondence should be addressed.
alu@mail.utexas.edu

[1] J. D. Jackson, *Classical Electrodynamics*, 3rd ed. (John Wiley & Sons, New York, 1999).
[2] L. Onsager, Reciprocal relations in irreversible processes. I., Phys. Rev. **37**, 405 (1931).
[3] L. Onsager, Reciprocal relations in irreversible processes. II., Phys. Rev. **38**, 2265 (1931).
[4] H. B. G. Casimir, On Onsager's principle of microscopic reversibility, Rev. Mod. Phys. **17**, 343 (1945).
[5] H. B. G. Casimir, Reciprocity theorems and irreversible processes, Proc. IEEE **51**, 1570 (1963).
[6] Z. Yu and S. Fan, Complete optical isolation created by indirect interband photonic transitions, Nat. Photonics **3**, 91 (2009).
[7] M. S. Kang, A. Butsch, and P. St. J. Russell, Reconfigurable light-driven optoacoustic isolators in photonic crystal fibre, Nat. Photonics **5**, 549 (2011).
[8] X. Huang and S. Fan, Complete all-optical silica fiber isolator via stimulated Brillouin scattering, J. Lightwave Technol. **29**, 2267 (2011).
[9] H. Lira, Z. Yu, S. Fan, and M. Lipson, Electrically Driven Nonreciprocity Induced by Interband Photonic Transition on a Silicon Chip, Phys. Rev. Lett. **109**, 033901 (2012).
[10] K. Fang, Z. Yu, and S. Fan, Photonic Aharonov-Bohm Effect Based on Dynamic Modulation, Phys. Rev. Lett. **108**, 153901 (2012).
[11] D.-W. Wang, H.-T. Zhou, M.-J. Guo, J.-X. Zhang, J. Evers, and S.-Y. Zhu, Optical Diode Made from a Moving Photonic Crystal, Phys. Rev. Lett. **110**, 093901 (2013).
[12] S. Qin, Q. Xu, and Y. E. Wang, Nonreciprocal components with distributedly modulated capacitors, IEEE Trans. Microwave Theory Tech. **62**, 2260 (2014).
[13] D. L. Sounas, C. Caloz, and A. Alù, Giant nonreciprocity at the subwavelength scale using angular momentum-biased metamaterials, Nat. Commun. **4**, 2407 (2013).
[14] R. Fleury, D. L. Sounas, C. F. Sieck, M. R. Haberman, and A. Alù, Sound isolation and giant linear nonreciprocity in a compact acoustic circulator, Science **343**, 516 (2014).
[15] D. L. Sounas and A. Alù, Angular-momentum-biased nanorings to realize magnetic-free integrated optical isolation, ACS Photonics **1**, 198 (2014).
[16] N. A. Estep, D. L. Sounas, J. Soric, and A. Alù, Magnetic-free nonreciprocity and isolation based on parametrically modulated coupled-resonator loops, Nat. Phys. **10**, 923 (2014).
[17] N. A. Estep, D. L. Sounas, and A. Alù, Magnetless microwave circulators based on spatiotemporally modulated rings of coupled resonators, IEEE Trans. Microwave Theory Tech. **64**, 502 (2016).
[18] S. Tanaka, N. Shimimura, and K. Ohtake, Active circulators—the realization of circulators using transistors, Proc. IEEE **53**, 260 (1965).
[19] Y. Ayasli, Field effect transistor circulators, IEEE Trans. Magn. **25**, 3242 (1989).
[20] T. Kodera, D. L. Sounas, and C. Caloz, Artificial Faraday rotation using a ring metamaterial structure without static magnetic field, Appl. Phys. Lett. **99**, 031114 (2011).
[21] T. Kodera, D. L. Sounas, and C. Caloz, Nonreciprocal magnetless CRLH leaky-wave antenna based on a ring metamaterial structure, IEEE Antennas Wireless Propag. Lett. **10**, 1551 (2011).
[22] T. Kodera, D. L. Sounas, and C. Caloz, Magnetless nonreciprocal metamaterial (MNM) technology: Application to microwave components, IEEE Trans. Microwave Theory Tech. **61**, 1030 (2013).
[23] Z. Wang, Z. Wang, J. Wang, B. Zhang, J. Huangfu, J. D. Joannopoulos, M. Soljačić, and L. Ran, Gyrotropic response in the absence of a bias field, Proc. Natl. Acad. Sci. U.S.A. **109**, 13194 (2012).
[24] B.-I. Popa and S. A. Cummer, Nonreciprocal active metamaterials, Phys. Rev. B **85**, 205101 (2012).
[25] See Supplemental Material at http://link.aps.org/supplemental/10.1103/PhysRevLett.118.154302 for detailed analytical derivations, which includes Refs. [1,26–28].
[26] K. X. Wang, Z. Yu, S. Sandhu, and S. Fan, Fundamental bounds on decay rates in asymmetric single-mode optical resonators, Opt. Lett. **38**, 100 (2013).
[27] *NIST Handbook of Mathematical Function*, edited by F. W. J. Olver, D. W. Lozier, R. F. Boisvert, and C. W. Clark (Cambridge University Press, New York, 2010).
[28] R. E. Colin, *Antennas and Radiowave Propagation* (McGraw-Hill, New York, 1985).
[29] H. Zhou, B. Zhen, C. W. Hsu, O. D. Miller, S. G. Johnson, J. D. Joannopoulos, and M. Soljačić, Perfect single-sided radiation and absorption without mirrors, Optica **3**, 1079 (2016).
[30] For two-dimensional objects, $\lambda^2/(4\pi)$ in Eq. (3) should be replaced by $\lambda/(2\pi)$.

[31] D. L. Sounas and A. Alù, Extinction symmetry for reciprocal objects and its implications on cloaking and scattering manipulation, Opt. Lett. **39**, 4053 (2014).
[32] A. Alù and N. Engheta, Achieving transparency with plasmonic and metamaterial coatings, Phys. Rev. E **72**, 016623 (2005).
[33] A. Alù, Mantle cloak: Invisibility induced by a surface, Phys. Rev. B **80**, 245115 (2009).
[34] J. C. Soric, P. Y. Chen, A. Kerkhoff, D. Rainwater, K. Melin, and A. Alù, Demonstration of an ultralow profile cloak for scattering suppression of a finite-length rod in free space, New J. Phys. **15**, 033037 (2013).
[35] X.-S. Lin, J.-H. Yan, L.-J. Wu, and S. Lan, High transmission contrast for single resonator based all-optical diodes with pump assisting, Opt. Express **16**, 20949 (2008).
[36] S. Manipatruni, J. T. Robinson, and M. Lipson, Optical Nonreciprocity in Optomechanical Structures, Phys. Rev. Lett. **102**, 213903 (2009).
[37] A. Miroshnichenko, E. Brasselet, and Y. S. Kivshar, Reversible optical nonreciprocity in periodic structures with liquid crystals, Appl. Phys. Lett. **96**, 063302 (2010).
[38] I. V. Shadrivov, V. A. Fedotov, D. A. Powell, Y. S. Kivshar, and N. I. Zheludev, Electromagnetic wave analogue of an electronic diode, New J. Phys. **13**, 033025 (2011).
[39] S. Lepri and G. Casati, Asymmetric Wave Propagation in Nonlinear Systems, Phys. Rev. Lett. **106**, 164101 (2011).
[40] S. V. Zhukovsky and A. G. Smirnov, All-optical diode action in asymmetric nonlinear photonic multilayers with perfect transmission resonances, Phys. Rev. A **83**, 023818 (2011).
[41] L. Fan, J. Wang, L. T. Varghese, H. Shen, B. Niu, Y. Xuan, A. M. Weiner, and M. Qi, An all-Silicon passive optical diode, Science **335**, 447 (2012).
[42] Y. Xu and A. E. Miroshnichenko, Reconfigurable nonreciprocity with a nonlinear Fano diode, Phys. Rev. B **89**, 134306 (2014).
[43] Y. Shi, Z. Yu, and S. Fan, Limitations of nonlinear optical isolators due to dynamic reciprocity, Nat. Photonics **9**, 388 (2015).